

$^{90}\text{Zr}(n,d)^{89}\text{Y}$  reaction at 22 MeV

K. Bharuth-Ram and A. C. Bawa

*Physics Department, University of Durban-Westville, Durban 4001, South Africa*

W. R. McMurray

*Van de Graaff Group, National Accelerator Centre, Faure 7131, South Africa*

(Received 13 April 1987)

The angular distribution of deuterons from the  $^{90}\text{Zr}(n,d)^{89}\text{Y}$  reaction at  $E_n=22$  MeV has been measured with a spectrometer consisting of three multiwire proportional counters followed by a curved plastic scintillator. Spectra were obtained with an energy resolution full width at half maximum, of about 0.7 MeV and an angle resolution full width at half maximum of about  $4^\circ$ . Two prominent peaks were observed in the spectra corresponding to transitions to the ground state and to two states at  $\sim 1.6$  MeV excitation in  $^{89}\text{Y}$ . Distorted wave Born approximation analysis of the angular distributions yielded spectroscopic factors of 1.7(5), 1.8(5), and 0.8(4), respectively, for the transitions to the ground state, the 1.51 MeV state, and the 1.75 MeV state. The results are compared with previous measurements and model predictions.

## I. INTRODUCTION

Theoretical and experimental interests in the nuclides around  $A=90$  stem from the fact that they comprise the lightest nuclei in which the valence protons and neutrons fill different shell model orbitals.<sup>1-3</sup> In the case of  $^{90}\text{Zr}$ , its shell model description consists of two valence protons outside the closed  $2p_{3/2}$  shell, i.e., coupled to an inert  $^{88}\text{Sr}$  core. The ground state configuration of  $^{90}\text{Zr}$  is shown in Fig. 1. Admixtures of  $J=0^+$  states of the  $(2p_{1/2})^2$  and  $(1g_{9/2})^2$  proton configurations lead to the  $0^+$  ground state and first excited state. The other low-lying levels arise from the  $(1g_{9/2})^2$  and  $(p_{1/2},g_{9/2})^2$  configurations.

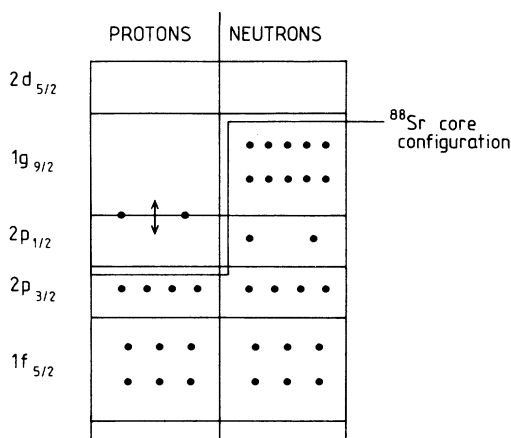
The low-lying states of  $^{89}\text{Y}$  have been described in terms of two models: in one these states are expected to arise from the extra proton outside the filled  $2p_{3/2}$  and  $1f_{5/2}$  subshells, while an alternative model of the low-lying  $\frac{3}{2}^-$  and  $\frac{5}{2}^-$  states describes them as proton holes in the  $2p_{3/2}$  and  $1f_{5/2}$  orbitals of  $^{90}\text{Zr}$ . Proton pickup reactions provide a convenient test of these shell model descriptions. Investigations via the  $(d,^3\text{He})$  reaction have yielded quite differing values for the spectroscopic factors for the transitions to the 1.51 MeV ( $\frac{3}{2}^-$ ) and the 1.75 MeV ( $\frac{5}{2}^-$ ) states in  $^{89}\text{Y}$ .<sup>4-6</sup> Further investigations have been carried out using the  $(^6\text{Li},^7\text{Be})$  reaction,<sup>7</sup> while the  $(e,e'p)$  reaction has been recently used to investigate the fragmentation of  $1f$ -hole strengths in  $^{90}\text{Zr}$ .<sup>8</sup> In this paper we report on the  $^{90}\text{Zr}(n,d)^{89}\text{Y}$  reaction, studied at  $E_n=21.8$  MeV.

Haight *et al.*<sup>9</sup> investigated the mechanisms by which  $(n, \text{charged particle})$  reactions induced by 15 MeV neutrons on  $^{90}\text{Zr}$  proceed. While the proton and alpha emissions were found to proceed mainly through compound nuclear processes, the deuteron emission displayed preequilibrium, most probably direct, reaction behavior. We therefore used a direct reaction analysis

on our measurements at 22 MeV, and derived spectroscopic factors for transitions to the ground state and excited states at  $\sim 1.6$  MeV in  $^{89}\text{Y}$ .

## II. EXPERIMENTAL DETAILS

The measurements of the deuteron cross sections were made with a spectrometer specifically designed for the study of neutron-induced reactions with low charged particle yields.<sup>10,11</sup> The spectrometer is shown schematically in Fig. 2. It consists of three multiwire proportional counters (A/Co, PC1, PC2) followed by a plastic scintillator. Neutrons with an energy of 21.8 MeV were produced via the  $(d,t)$  reaction with 5.25 MeV deuterons incident on a tritium gas cell. The target sample was positioned 12.0 cm from the center of the tritium cell. It was in the form of a  $15 \text{ mg cm}^{-2}$  foil enriched to 97%  $^{90}\text{Zr}$  with an effective surface area of  $1.0 \times 1.0 \text{ cm}$ , and was sandwiched between proportional counters A/Co and PC1. The proportional counters were operated in a continuous flow mode with a 10%  $\text{CH}_4/90\%$  Ar gas mixture. A/Co was operated in anticoincidence, and PC1 and PC2 in coincidence with the scintillator to select only events originating in the target sample. Counters PC1 and PC2 act as two " $\Delta E$ " detectors, and the scintillator as an energy " $E$ " detector, thus providing  $\Delta E$ - $E$  particle identification. The plastic scintillator (5 mm thick, 50 mm high, and 300 mm long) is shaped into a curve with a radius of 200 mm, and is viewed by two photomultipliers,  $A$  and  $B$ . The energy signal  $E$  is obtained by summing the outputs  $A$  and  $B$ , and the position (i.e., nominal angle) information from the function  $(A-B)/(A+B)$ , which was found to vary nearly linearly with position along the scintillator. The outputs  $A$  and  $B$  were matched, and the position sensitivity was calibrated using a 1 MeV conversion electron source ( $^{207}\text{Bi}$ ). The spectrometer thus provides particle identification and background suppression, and allows

FIG. 1. Ground state configuration of  $^{90}\text{Zr}$ .

the simultaneous accumulation of data over an angle range of  $80^\circ$  with an angular resolution of  $\approx 4^\circ$  full width at half maximum (FWHM). The raw data outputs  $A$  and  $B$  from the scintillator, and  $C_1$  and  $C_2$  from the proportional counters, were gated by the coincidence-anticoincidence requirements and accumulated in a multiparameter mode on a buffer tape. The data were analyzed with the aid of a program which was used to compute the angle of detection, make corrections to the input parameters, set particle identification limits on  $\Delta E$ - $E$  displays, and scan the data for the energy or angle spectra of all events in specified deuteron loci and angle or energy limits.

The detection system was checked by observing recoil protons from a thin polythene sample with a coating of carbon to provide conducting walls for the proportional counters. A similar deuterated polythene sample was used to check the efficacy of the particle identification. The recoil particle spectra were used to check the efficiency of the spectrometer and to provide the normalization for the (n,d) reaction cross sections.

Operating the proportional counter sandwich without

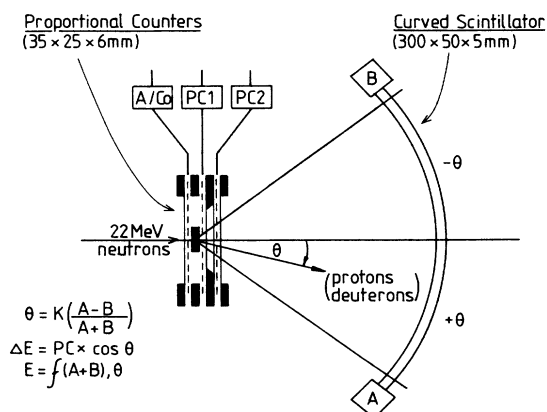


FIG. 2. A schematic representation of the spectrometer.

a wall between the anticoincidence counter and its adjacent one produced spectra from conducting foil samples that were essentially free of reaction background. The background from the counter gas was checked during runs with target-in and target-out measurements.

Deuteron spectra from the  $^{90}\text{Zr}(n,d)^{89}\text{Y}$  reaction were generated for nominal scattering angles  $2.5^\circ$ ,  $7.5^\circ$ ,  $12.5^\circ$ ,  $22.5^\circ$ ,  $27.5^\circ$ ,  $35^\circ$ , and  $50^\circ$  with a nominal angle spread of  $5^\circ$ . Calculations of the angle resolution functions, allowing for the extended neutron source, the finite target dimensions, and the scintillator height, showed that these angles in fact correspond to mean scattering angles  $6.0^\circ$ ,  $9.1^\circ$ ,  $13.5^\circ$ ,  $18.2^\circ$ ,  $23.1^\circ$ ,  $28.0^\circ$ ,  $35.4^\circ$ , and  $50.2^\circ$ , respectively, with a full angle spread at half maximum of about  $8^\circ$ . Figure 3 shows a deuteron spectrum integrated over the angle range  $-30^\circ$  to  $+30^\circ$  relative to the direction of the incident beam. Two prominent peaks are seen, corresponding to transitions to the ground state and to states at  $\sim 1.6$  MeV excitation in  $^{89}\text{Y}$ . There is also evidence of excitation of higher energy states.

### III. DISTORTED WAVE ANALYSIS

The comparisons between the experimental and theoretical cross sections were carried out via the relationship

$$\sigma(\theta)_{\text{expt}} = \frac{1}{2} D_0^2 (C^2 S) \sigma(\theta)_{\text{DWBA}},$$

where DWBA denotes distorted wave Born approximation. The value of the overlap integral  $D_0^2$  was taken to be 1.55 from calculations which included the effect of  $d$ -state admixture in the deuteron wave function.<sup>12</sup> The quantity  $C^2 S$ , where  $\langle C \rangle = \langle T_f T_{fz} \frac{1}{2} t_z | T_i T_{iz} \rangle$ , is the isospin Clebsch-Gordan coefficients with  $T_i$  and  $T_f$  being the isospins of the initial and final nuclei, is then the spectroscopic factor. The DWBA calculations were performed in the local energy approximation (LEA) which includes corrections both for finite range and nonlocality of the optical model potential. The calculations were performed with the code DWUCK4 (Ref. 13) with an optical potential of the form

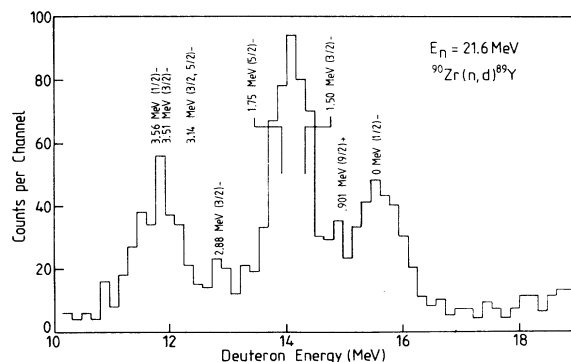
FIG. 3. Deuteron spectrum from the  $^{90}\text{Zr}(n,d)^{89}\text{Y}$  reaction, integrated over an angle range from  $-30^\circ$  to  $+30^\circ$ . A small proton background ( $< 10\%$ ) underlies the spectrum.

TABLE I. The optical model and bound state parameters.

	$V_0$ (MeV)	$r_R$ (fm)	$a_R$ (fm)	$W_0$ (MeV)	$r_w$ (fm)	$a_w$ (fm)	$W_d$ (MeV)	$r_d$ (fm)	$a_d$ (fm)	$V_{SO}$ (MeV)	$r_{SO}$ (fm)	$a_{SO}$ (fm)	$r_c$ (fm)
n <sup>a</sup>	46.7	1.17	0.75	3.19	1.26	0.58	6.2	1.26	0.58	6.2	1.01	0.75	
d <sup>b</sup>	92.1	1.17	0.74	2.97	1.33	0.80	12.3	1.33	0.80	6.9	1.07	0.66	1.3
p <sup>a</sup>	c	1.17	0.75							6.2	1.01	0.75	1.3

<sup>a</sup>Reference 11.

<sup>b</sup>Reference 12.

<sup>c</sup>Potential depth adjusted to give correct binding energy [  $|B_n| = |B_n(\text{g.s.})| + E_{Ex}$  ].

$$\begin{aligned}
 V(r) = & -V_0 f(r, r_R, a_R) - iW_0 f(r, r_w, a_w) \\
 & + i4W_d \frac{d}{dr} f(r, r_d, a_d) \\
 & + V_{SO} \frac{1}{r} \frac{d}{dr} f(r, r_{SO}, a_{SO}) \mathbf{L} \cdot \mathbf{s} + V_c(r),
 \end{aligned}$$

where the Woods-Saxon form factor of the potential well is given by

$$f(r, r_i, a_i) = \{1 + \exp[(r - r_i A^{1/3})/a_i]\}^{-1}.$$

The Coulomb potential  $V_c(r)$  is approximated by the potential due to a uniformly charged sphere of radius  $r_c A^{1/3}$ . The imaginary part of the potential could be fixed to either pure volume ( $W_0 \neq 0$ ,  $W_d = 0$ ) or pure surface ( $W_0 = 0$ ,  $W_d \neq 0$ ).

Data on optical model analyses of elastic scattering of 21.8 MeV neutrons from  $^{90}\text{Zr}$  and 13–15 MeV deuterons from  $^{89}\text{Y}$  is scarce. Hence the parameters used in the present calculations were derived from global parameter sets.<sup>14–16</sup> The parameters are listed in Table I. Finite range corrections in these calculations were within the LEA, with the finite range parameter set to 0.667. The parameters to minimize the effects of nonlocality of the potential were set at their usual value of  $\beta = 0.85$  for nucleons and  $\beta = 0.54$  for deuterons.<sup>17</sup>

Least squares fits to the experimental cross sections were obtained by minimizing the expression

$$\chi^2 = \frac{1}{N} \sum_i \frac{[N' C^2 S \sigma(\theta_i)_{\text{DWBA}} - \sigma(\theta_i)_{\text{expt}}]^2}{\Delta \sigma(\theta_i)_{\text{expt}}^2}.$$

The deuteron angular distributions are shown in Fig. 4, together with DWBA fits in which the  $^{90}\text{Zr}$  ground state was taken to be a mixed configuration

$$\psi(0) = a\psi(p_{1/2})^2 - b\psi(g_{9/2})^2, \quad a^2 = 0.7 \text{ and } b^2 = 0.3.$$

The ground state peak in the deuteron spectrum corresponds to a residual nucleus spin  $J^\pi = \frac{1}{2}^-$ . This corresponds to the pickup of a valence proton from the  $2p_{1/2}$  shell model orbital in  $^{90}\text{Zr}$ . The proton occupancy of this orbital is 1.33.<sup>3</sup> Fitting an  $l=1$  distribution to the experimental points gives a spectroscopic factor of  $1.8 \pm 0.5$ . As the energy resolution of the spectrometer is  $\sim 0.6$  MeV (FWHM) it is likely that the “ground state” peak contains some contribution from proton pickup leading to population of the first excited state in  $^{89}\text{Y}$  at 0.91 MeV (see Fig. 3). Indeed, a direct transition to this level is obtained from a pickup of one of the valence protons in the  $^{90}\text{Zr}$   $1g_{9/2}$  orbital. Taking account of this contribution does improve the fit to the experimental cross sections, with the best fit being obtained with only a 15% contribution. This is shown in Fig. 4. The spectroscopic factor then obtained for the transition to the

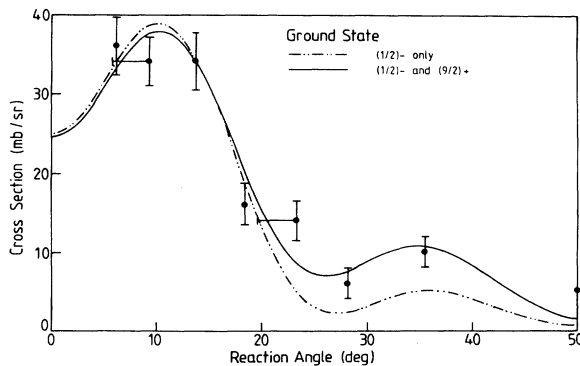


FIG. 4. Angular distribution of deuterons corresponding to transitions to the  $^{89}\text{Y}$  ground state. The curves represent DWBA fits (see text).

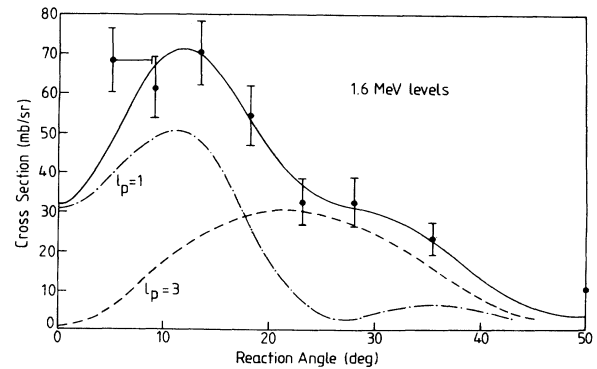


FIG. 5. Angular distribution of deuterons corresponding to transitions to the 1.51 MeV ( $\frac{3}{2}^-$ ) and 1.75 MeV ( $\frac{5}{2}^-$ ) levels in  $^{89}\text{Y}$ . The dashed curves represent the distributions for  $l=1$  and  $l=3$  transfer; the solid curve represents the summed DWBA fit to the data.

TABLE II. Comparison of spectroscopic factors.

$E_x$ (MeV)	$J^\pi$	$l$	Present work	$C^2S$							Model
				a	b	Previous work			d	e	
0.0	$\frac{1}{2}^-$	1	1.7(5)	1.41	1.91	2	1.8	2	1.1	2.9	1.4
0.91	$\frac{9}{2}^+$	4		0.51	1.10		1.25		0.6		0.6
1.51	$\frac{3}{2}^-$	1	1.8(5)	2.2	4.25	2.8	3.9	2.6	2.1		4
1.75	$\frac{5}{2}^-$	3	0.8(4)	2.0	7.80	5.2	8.9	5.8	5.2		6

<sup>a</sup>Kovaloski *et al.* (1967): (d,<sup>3</sup>He).

<sup>b</sup>Preedom *et al.* (1968): (d,<sup>3</sup>He).

<sup>b'</sup>Normalized values of footnote b (see text).

<sup>c</sup>Stuirbrink *et al.* (1980): (d,<sup>3</sup>He).

<sup>c'</sup>Normalized values of footnote c (see text).

<sup>d</sup>Wadsworth *et al.* (1983): (<sup>6</sup>Li,<sup>7</sup>Be).

<sup>e</sup>den Herder *et al.* (1985): (e,e'p).

<sup>89</sup>Y ground state is  $1.7 \pm 0.5$ . The "1.6 MeV" peak contains deuterons corresponding to transitions to the second and third excited states in <sup>89</sup>Y at 1.51 MeV and 1.75 MeV. Deuterons populating the fourth excited state at 2.22 MeV could be present in the tail of the "1.6 MeV" peak. However, this state has  $J^\pi = \frac{5}{2}^+$  and is unlikely to be excited in the (n,d) reaction since the  $2d_{5/2}$  orbital in <sup>90</sup>Zr has zero proton occupancy. The 1.51 MeV and 1.75 MeV levels have  $J^\pi = \frac{3}{2}^-$  and  $\frac{5}{2}^-$ , respectively, corresponding to proton transfers from the  $2p_{3/2}$  and  $1f_{5/2}$  orbitals in <sup>90</sup>Zr. The angular distribution for the sum of the reactions to these two levels is consequently very sensitive to their relative excitation intensity (see Fig. 5). This makes it possible to determine separate spectroscopic values. The spectroscopic factors derived from the analysis are listed in Table II. The error in the spectroscopic factors are set at 30%, taking into account a 15% experimental error and a 25% error on the Bassel normalization factor.

#### IV. RESULTS AND DISCUSSION

The spectroscopic factor determined in the present work are compared in Table II with previous measurements and the shell model limits. Our spectroscopic factor for the  $l=1$  transition to the <sup>89</sup>Y ground state agrees well with previous measurements, and within error, with the model limit.

The spectroscopic factor of 1.8(6) for the transition to the 1.51 MeV state is in very good agreement with the (d,<sup>3</sup>He) measurement of Kovaloski *et al.*,<sup>4</sup> and the (<sup>6</sup>Li,<sup>7</sup>Be) measurement of Wadsworth *et al.*<sup>7</sup> At first sight our results and those of Refs. 4 and 7 appear to be in disagreement with the (d,<sup>3</sup>He) measurements of Preedom and Newman<sup>5</sup> and Stuirbank.<sup>6</sup> However, when the results are normalized so that the proton pickup strengths for the transitions to the ground state and the  $g_{9/2}$  first excited state add up to the model limit of 2 (columns b' and c' in Table II), the spectroscopic factors of these authors reduce to 2.8 and 2.6, respectively (and ours increases to 2.1), which then bring all the measurements into reasonable agreement.

Our results, combined with the previous measurements, suggest that the wave function for the 1.51 MeV state in <sup>89</sup>Y contains about 60% of the  $(p_{3/2})^{-1}$  hole strength. However, Kovaloski *et al.*<sup>4</sup> have pointed out that the  $(p_{1/2})^2-(g_{9/2})^2$  mixing is unlikely to be identical for <sup>89</sup>Y and <sup>90</sup>Zr. Assuming that the paired proton in <sup>89</sup>Y were in the  $(2p_{1/2})^2$  configuration only, reduces the model spectroscopic factor to 2.8.<sup>4</sup> In such a case the single hole strength in the <sup>89</sup>Y 1.51 MeV state would amount to about 80%.

For the transition to the 1.75 MeV,  $\frac{5}{2}^-$  state we obtain a value of  $C^2S=0.8(4)$ , which is very much lower than any of the previous measurements and the model limit. We do not have a ready explanation for this discrepancy, nor are we able to explain the large discrepancy between the (d,<sup>3</sup>He) measurements which yield  $C^2S$  values ranging from 2.0 to 8.9 (5.8). As stated already, the spectroscopic factor for the transition to this state has been obtained from a simultaneous  $l=1$  plus  $l=3$  analysis of the unresolved "1.6" MeV deuteron peak. Even allowing extreme values in the experimental error and overestimation of the  $l=1$  contribution in the angular distribution (see Fig. 5) is unable to account for the low  $l=3$  strength we obtain. A possible explanation may be that the  $1f$ -hole strength is fragmented over several MeV. Our summed deuteron spectrum does show evidence of excitation of higher  $\frac{3}{2}^-$  and  $\frac{5}{2}^-$  states. Indeed summing events for each  $\Delta E=0.7$  MeV bin separately does show additional  $l=3$  type distribution. However, the statistics are too poor for a DWBA analysis. Strong evidence for the fragmentation of the  $1f$ -hole strength has recently been obtained from <sup>90</sup>Zr(e,e'p) measurements which shows the  $1f$  strength to extend beyond 10 MeV excitation energy.<sup>8,18</sup> The (e,e'p) measurements give a total  $1f$  strength below 9 MeV of  $\sum C^2S=8$ , which is much lower than the sum rule value of 14.

Further evidence of a strong fragmentation of the  $f_{5/2}$  hole strength comes from the <sup>116</sup>Sn(d,<sup>3</sup>He)<sup>115</sup>In measurements of Hesselink *et al.*<sup>19</sup> The spectroscopic factors deduced by these authors for  $p_{1/2}$ ,  $p_{3/2}$ , and  $f_{5/2}$  proton pickup to the first three excited states of <sup>115</sup>In are 1.7,

2.0, and 0.7, respectively, which are similar to our values. While this agreement is perhaps fortuitous, the occupancy of the  $p_{3/2}$  and  $f_{5/2}$  shells in  $^{116}\text{Sn}(Z=50)$  and  $^{90}\text{Zr}(Z=40)$  are the same, and the pickup strengths from these shells in the two nuclei, to a first approximation, are expected to be similar. Our measurements appear to support this.

#### ACKNOWLEDGMENTS

The authors thank R. Verbruggen and T. Swart for construction of the spectrometer, J. Pilcher for the software for data reduction, and the accelerator operating staff for excellent support.

- 
- <sup>1</sup>I. Talmi and I. Unna, Nucl. Phys. **19**, 225 (1966).  
<sup>2</sup>N. Auerbach and I. Talmi, Nucl. Phys. **64**, 458 (1965).  
<sup>3</sup>D. H. Gloeckner, Nucl. Phys. **A253**, 301 (1975).  
<sup>4</sup>C. K. Kovaloski, J. S. Lilley, D. C. Shreve, and N. Stein, Phys. Rev. **161**, 1107 (1967).  
<sup>5</sup>B. M. Preedom and E. Newman, Phys. Rev. **166**, 1156 (1968).  
<sup>6</sup>A. Stuirbank, Z. Phys. A **297**, 307 (1980).  
<sup>7</sup>R. Wadsworth, M. D. Cohler, M. J. Smithson, D. L. Watson, F. Jundt, L. Kraus, I. Linck, and J. C. Sens, J. Phys. G **9**, 1237 (1983).  
<sup>8</sup>J. W. A. den Herder, P. C. Dunn, E. Jans, P. H. M. Keizer, L. Lapikas, E. N. M. Quint, P. K. A. de Witt Huberts, H. P. Blok, and G. van der Steenhoven, Phys. Lett. **161B**, 65 (1985).  
<sup>9</sup>R. C. Haight, S. M. Grimes, R. G. Johnson, and H. H. Barschall, Phys. Rev. C **23**, 700 (1981).  
<sup>10</sup>W. R. McMurray and K. Bharuth-Ram, S. Afr. J. Phys. **8**, 22 (1985).  
<sup>11</sup>W. R. McMurray, K. Bharuth-Ram, and S. M. Perez, Z. Phys. A **315**, 189 (1984).  
<sup>12</sup>C. B. Fulmer and J. B. Ball, Phys. Rev. **140**, B330 (1965).  
<sup>13</sup>P. D. Kunz, University of Colorado, 1978 (unpublished).  
<sup>14</sup>P. G. Roos, S. M. Smith, V. K. C. Cheng, G. Tibbel, A. A. Cowley, and R. A. J. Riddle, Nucl. Phys. **A255**, 187 (1975).  
<sup>15</sup>W. W. Daehnick, J. D. Childs, and Z. Vreelz, Phys. Rev. C **21**, 2253 (1980).  
<sup>16</sup>F. D. Becchetti and G. W. Greenlees, Phys. Rev. **182**, 1190 (1969).  
<sup>17</sup>R. H. Bassel, Phys. Rev. **149**, 791 (1966).  
<sup>18</sup>L. Lapikas, Nucl. Phys. **A434**, 85c (1985).  
<sup>19</sup>W. H. A. Hesselink, B. R. Kooistra, L. W. Put, R. H. Siemssen, and S. Y. van der Werf, Nucl. Phys. **A226**, 229 (1974).